Dose Escalation Biodistribution, Positron Emission Tomography/Computed Tomography Imaging and Dosimetry of a Highly Specific Radionuclide-labeled Non-blocking Nanobody

Yang yanling (✉ yl.yang@smartnucl.com)

  Yantai University   https://orcid.org/0000-0003-0434-9384

Feng Zhao

  Yantai University

Daquan Chen

  Yantai University

Chao Wang

  SmartNuclide biopharma Co.Ltd

Yan Sun

  SmartNuclide Biopharma

Tao Xu

  SmartNuclide Biopharma

Hui Xu

  Yantai University

Huaying Fan

  Yantai University

Abstract

Background: Immunotherapy is a valuable option for the treatment of cancers, and the curative effect anti-PD-1/PD-L1 therapy correlates closely with PD-L1 expression levels. Positron emission tomography (PET) imaging of PD-L1 expression is feasible using ^{68}Ga-NOTA-Nb109 nanobodies. ^{68}Ga-NOTA-Nb109 was generated by radionuclide (^{68}Ga) labeling of Nb109 using a NOTA chelator. To facilitate clinical trials, We explored the optimal dose range of ^{68}Ga-NOTA-Nb109 in BALB/c A375-hPD-L1 tumor-burdened nude mice and C57-hPD-L1 transgenic MC38-hPD-L1 tumor-burdened mice by intravenous of a single intravenous dose of ^{68}Ga-NOTA-Nb109 and confirmed the dose in cynomolgus monkeys. The biodistribution data of cynomolgus monkey PET images were extrapolated to estimate the radiation dose for the adult male using OLINDA2.1 software.

Results: ^{68}Ga-NOTA-Nb109 was stable in physiologic media and human serum. Ex vivo biodistribution studies showed rapid and specific uptake in A375-hPDL1 or MC38-hPDL1 tumors. The estimated ED_{50} was approximately 5.4 μg in humanized mice. The injected mass (0.3–100 μg in nude mice and approximately 1–100 μg in humanized mice) greatly influenced the general biodistribution, with a better tumor-to-background ratio acquired at lower doses of Nb109 (0.3–10 μg in nude mice and approximately 1 μg in humanized mice), indicating maximum uptake in tumors at administered mass doses below the estimated ED_{50}. Therefore, a single 15 μg/kg dose was adopted for the PET/CT imaging in cynomolgus monkey. The highest specific and persistent uptake of the tracer was detected in the spleen, with the exception of the levels in the kidney and urine bladder, which was related to metabolism and excretion. The spleen-to-muscle ratio of the tracer exceeded 10 from immediately to 4 h after administration, indicating that the dose was appropriate. The estimated effective dose was calculated to yield a radiation dose of 4.1 mSv to a patient after injection of 185 MBq of ^{68}Ga-NOTA-Nb109.

Conclusion: ^{68}Ga-NOTA-Nb109 showed specific accumulation in hPD-L1 xenografts in ex vivo biodistribution studies and monkey PET/CT imaging. The dose escalation distribution data provided a recommended dose range for further use, and the safety of the tracer was confirmed in dosimetry studies.

Background

The Global Cancer Statistics report estimated that there were 18.1 million new cancer cases and 9.6 million cancer deaths in 2018, with over 50% of the cancer deaths in occurring in Asia [1]. A new report predicts a 60% increase in the global number of cancer cases within the next two decades, with lung cancer continuing to be the leading cause of cancer deaths [2]. Immunotherapies, especially inhibitors targeting programmed cell death protein 1 (PD-1) or its ligand (PD-L1), have become a focus of cancer research in recent years. However, the PD-L1 status of the tumor is correlated with the outcome of PD-1:PD-L1 blockade occurring outside the tumor microenvironment.

In recent years, tracers for radioimmune-imaging have provided a non-invasive alternative to traditional immunohistochemical (IHC) staining for monitoring of PD-L1 expression. Although ^{18}F-

fluorodeoxyglucose (^{18}F-FDG) is the most commonly used radioactive tracer, its uptake is not tumor cell-specific and it can also be taken up by activated immune cells [3]. Thus, several specific imaging agents, including monoclonal antibodies (mAbs; such as ^{89}Zr-avelumab[4], ^{89}Zr-atezolizumab[5], ^{89}Zr-nivolumab[6]), mAb fragments (such as minibodies and nanobodies [7, 8]), small proteins (such as ^{18}F-BMS-986192 [6, 9]), and peptides (such as ^{64}Cu-WL12 [10]), have been developed and investigated in preclinical models in addition to some early clinical studies.

Although the high specificity, affinity, and ready availability of full-length IgG antibodies provides some feasibility for imaging, the characteristics of mAb metabolism in liver lead to high uptake of radioactivity in the liver, and their large size (approximately 150 kD) limits tissue penetration, tumor retention and clearance from the circulation. Furthermore, the long half-lives of these proteins means that high-contrast images cannot be obtained in a short timeframe (several days are required) [11, 12]. To overcome these challenges, peptides and smaller antibody fragments (approximately 10 kD) have been developed for in vivo imaging. These agents provide superior imaging characteristics, such as rapid clearance from the circulation, higher tissue penetration, and higher signal-to-background ratios [8].

The protein dose has an important influence on imaging. The uptake of ^{68}Ga-DOTA-TOC improved in the neuroendocrine tumour and decreased in liver and spleen as the peptide dose increased to 50 μg, whereas the uptake decreased in the lesions and healthy organs with further elevation of the peptide dose to 500 μg [13]. The ratio of the lesion-to-liver uptake of ^{68}Ga-ABY-025 was higher with a high peptide dose (427 μg) than with the low peptide dose (78 μg)[14]. The spleen, blood and tumor uptake of ^{111}In-DTPA-anti-PD-L1 were significantly altered in the presence of excess (30- or 100-fold) unlabeled anti-PD-L1 mAb (spleen and blood, $P \le 0.0002$; tumor, $P \le 0.05$; all relative to the unblocked control) [15]. In a study of the PD-L1 targeting tracer ^{64}Cu-WL12, the imaging and biodistribution data showed high uptake in the tumor after pretreatment with low doses (0.06 mg/kg) of the anti-PD-L1 mAb, atezolizumab, compared with that at the higher doses of the mAb (0.6 and 3.6 mg/kg) [16]. These findings indicate that the signal-to-background uptake was high relative to the unlabeled dose of the protein.

Nanobodies, also known as single domain antibodies, are small proteins (approximately 15 kDa). As a result of the suitable configuration of The conformation of the complementarity determining regions confer nanobodies with many features that are for imaging applications, such as rapid targeting and blood clearance, high solubility, and stability, ease of cloning, and the capacity to bind to cavities and difficult-to-access antigens [17].

Nb109 is a non-blocking nanobody with high specific affinity for PD-L1 (with an equilibrium dissociation constant (K_D) of 2.9×10^{-9} M) [18, 19]. The epitope to which by Nb109 binds differs from those bound by the therapeutic PD-1 and PD-L1 antibodies. After conjugation with the chelator 1,4,7- triazacyclononane-1,4,7-triacetic acid (NOTA) and labeling with the radionuclide ^{68}Ga, ^{68}Ga-NOTA-Nb109 can bind with PD-L1 *in vivo*, and accumulates specifically in locations with high PD-L1 expression, such as the A375-hPD-L1 tumor. The uptake ratio is associated with the PD-L1 expression level. In addition to the uptake in the

tumor, the kidney showed relatively high uptake compared with the liver and other organs (33.7% vs. 1.1 % and < 1.5% ID/g, where ID%/g refers as the percentage injected dose per gram in each organ tissue).

In this study, we explored the suitable dose of ^{68}Ga-NOTA-Nb109 by comparing the effect of the injected mass on the biodistribution in two strains of mice (including humanized mice), and conducted positron emission tomography/computed tomography (PET/CT) imaging in non-human primates to further verify the dose of ^{68}Ga-NOTA- Nb109 based on the protein mass dose range determined. The biodistribution data of cynomolgus monkey were extrapolated to estimate the radiation dose for the adult male.

Material And Methods

All commercially obtained chemicals were of analytic grade, and all reagents were obtained from Sinopharm (Shanghai,China) unless otherwise stated. p-SCN-Bn-NOTA was purchased from Macrocyclics (USA). ^{68}Ga was obtained from a ^{68}Ga/^{68}Ge generator (ITG) and eluted with 0.1 M hydrochloric acid (HCl, Merck). High performance liquid chromatography (HPLC) was performed using e2695 HPLC (Waters) and thin layer chromatography (TLC) was performed on a Mini-scan TLC scanner (Eckert & Ziegler Radiopharma).

Production and purification of Nb109

The anti-PDL1 nanobody Nb109 was produced as described previously [18, 19].

Conjugation of p-SCN-Bn-NOTA to the nanobody

Nb109 was produced as described previously [19]. Nb109 (5 mg/mL) in 0.5 M sodium carbonate buffer (pH 9.8) was added to p-SCN-Bn-NOTA (6-fold molar excess) and incubated for 24 h at 30°C. The conjugate was then purified and the concentration of NOTA-Nb109 was determined using the DAR (Drug-to-antibody ratio, also refers as the number of chelates per nanobody). Nb109 activity was evaluated by enzyme-linked immunosorbent assay (ELISA).

Synthesis of ^{68}Ga-NOTA-Nb109

Briefly, using HCl as the eluent, the ^{68}Ga radionuclide was eluted from a ^{68}Ga/^{68}Ge generator (Germany, ITG). The precursor (NOTA-Nb109) was mixed with ^{68}Ga^{3+} in a acetate reaction system (pH 4.0−4.5), and incubated at room temperature to obtain a ^{68}Ga-NOTA-Nb109 injection sample. After the reaction was completed, sodium acetate solution was added to pH 5.5. Finally, the solution was filtered through 0.22-μm sterile filter membrane. The radiochemical purity and the stability of ^{68}Ga-NOTA-Nb109 were measured by radio-TLC or radio-HPLC.

In the dose escalation distribution study, the activity-to-volume ratio of the sample was calculated. The mass of Nb109 in the dosing solution was determined by the specific activity.

Cell lines and animals

The A375-PD-L1 and MC38-PD-L1 cell lines were generated by lentivirus infection and kindly provided by SmartNuclide Biopharm (China). Cells were cultured, and the PD-L1 expression level was confirmed via flow cytometry and immunohistochemical staining as described previously [19].

Female BALB/c nude mice and female C57-hPD-L1 transgenic mice were purchased from Gem Pharmatech Co., Ltd and ShangHai Model Organisms, respectively. The mice were subcutaneously inoculated at the left axilla with A375-PD-L1 (5×10^6 per mouse) or MC38-PD-L1 (0.5×10^6 per mouse), respectively. The tumors were allowed to grow for 1−2 weeks to approximately 100 mm^3.

Cynomolgus monkey studies were conducted in collaboration with WuXi AppTec (Shanghai,China) and Suzhou University-SmartNuclide Radiopharmaceutical Collaborative Innovation Center(Suzhou, China).

Ex vivo biodistribution in BALB/c nude mice

Female BALB/c A375-hPD-L1 tumor-burdened nude mice were injected with 0.3−1.2 MBq ^{68}Ga-NOTA-Nb109 via the tail vein, As described previously, the protein quantity was adjusted by dilution of the starting labeled preparation (^{68}Ga-NOTA-Nb109) with NOTA-Nb109 or normal saline to provide tracer doses containing 0.3 μg, 1 μg, 10 μg and 100 μg (n = 6 for each subgroup). At 1.5 h after dosing, the mice were sacrificed to collect tumors and other organs, which were washed, weighed immediately, and assessed with a gamma counter. Tumor and tissue or organ uptake were calculated as the percentage of injection dose per gram of tissue (%ID/g) and corrected for decay.

Ex vivo biodistribution and micro-PET imaging in humanized mice

To further explore the influence of injected tracer mass on specific uptake in normal and tumor tissues in the humanized system, the biodistribution of ^{68}Ga-NOTA-Nb109 containing four different quantities of protein was evaluated in MC38-hPD-L1 xenografts in C57-hPD-L1 transgenic mice at 1.5 h post-injection.

Female C57-hPD-L1 transgenic tumor-burdened mice were intravenously injected with 3−3.5 MBq of ^{68}Ga-NOTA-Nb109 in conjunction with escalating doses of unlabeled NOTA-Nb109 (1 μg, 10 μg, 50 μg and 100 μg per animal, n = 3 for each subgroup). At 1.5 h after dosing, the mice were sacrificed and tumors and tissue or organ uptake (%ID/g) was calculated and corrected for decay.

In addition, blood samples were collected from each animal 1.5 h post-dose were collected and analyzed for Nb109 concentrations (ng/mL) using a microplate reader (SpectraMax Plus190, Molecular Devices).

An additional tumor-bearing animal in each dose group was anesthetized with isoflurane and injected with 4.0−5.5 MBq tracers for dynamic whole-body PET scans (approximately 3 h) using a micro-PET scanner (Siemens Medical Solutions, Germany). Seventeen frame dynamic emission images were collected at 10-min intervals. The uptake of tracers in tumor or muscle (%ID/g) was estimated by sketching the region of interest (ROI) on images using ASIPro VM™ software (Siemens Medical Solutions, USA).

Cynomolgus monkey PET/CT imaging

A male healthy cynomolgus monkey was anesthetized by intramuscular injection of 0.3 mL/kg ketamine and transferred to the PET/CT scanner (PSTE16, GE Healthcare). After administration of ^{68}Ga-NOTA-Nb109 (approximately 30 MBq, 15 μg/kg) via the superficial vein, whole body PET/CT scanning was performed on the cynomolgus monkey under anesthesia with 0.75 mg/kg xylarizonaine. Emission images were acquired in a sequence of five passes over the previous five bed positions (5 min per position), producing a series of whole-body images covering a period of approximately 240 min after tracer administration.

After the scan, the PET-CT images (immediately, 15 min, 30 min, 1 h, 1.5 h, 2 h, and 4 h post-dose) were reconstructed iteratively. The reconstructed image was processed using medical analysis software PMOD to outline the ROI in tissues such as heart, lung, liver, kidneys, spleen, brain, muscle and bladder. The SUV (standard uptake value) in the ROI region was calculated.

Furthermore, blood samples were collected pre-dose and 5 min, 15 min, 30 min, 1 h, 1.5 h, 2 h, 3 h and 4 h post-dose for determination of blood radioactivity using a gamma counter (PE 2480). The remaining blood samples were then centrifuged at 4°C to obtain serum for Nb109 concentration (ng/mL) analyses by ELISA. The absorbance in each well was measured at 450/650 nm using a microplate reader (SpectraMax Plus190, Molecular Devices). Intact ^{68}Ga-NOTA-Nb109 signals in serum samples (approximately 100 μL) isolated from blood samples collected at 15 min, 30 min, and 1 h post-dose were subjected to radio-HPLC analyses. The concentration of free NOTA in serum samples (pre-dose and 5 min and 4 h post-dose) was detected by LC-MS.

Results

Synthesis of ^{68}Ga-NOTA-Nb109

The radiochemical purity of ^{68}Ga-NOTA-Nb109 measured by radio-TLC exceeded 95%. The in vitro stability of ^{68}Ga-NOTA-Nb109 in human serum and 0.9% NaCl solution was demonstrated by the radiochemical purity >95% over a period of 4 h at <25°C (Supplemental Figure 1).

Ex vivo distribution in rodents

Distribution in BALB/c nude mice.

After a single intravenous dose of ^{68}Ga-NOTA-Nb109 in BALB/c-A375-hPDL1 model mice, analysis of the uptake in each group showed specific binding in A375-hPDL1 tumors and the greatest uptake of the tracer (ID%/g) occurred in the kidney.

The A375-hPDL1 tumor-to-muscle ratio in the 0.3–10 μg/animal dose group was approximately 2.5–3.5 times greater than that in the 100 μg/animal dose group. In addition, the tumor-to-organ ratio changed (heart increased; lung, liver, spleen and kidney decreased) in a dose-dependent manner in the 0.3–10 μg/animal group, while a decrease in the uptake in tumors was observed in the 100 μg/animal group (Figure 1). These findings indicated that PD-L1binding was blocked by an excess of unlabeled NOTA-Nb109.

Distribution in C57-hPD-L1 transgenic mice.

The tumor-to-organ (heart, lungs, spleen, and liver) radioactivity ratios decreased progressively with increasing amounts of unlabeled NOTA-Nb109 (1–100 μg). The tumor-to-muscle ratio decreased by 2.5-fold, the tumor-to-lungs ratio decreased by 3.5- fold, and the tumor-to-other organs decreased by approximately 2-fold (Figure 2a), indicating specific binding of the tracer to PD-L1 in humanized mice. Based on the tumor-to-muscle ratio of the four groups, the estimated half-maximal effective dose (ED_{50}) was 5.4 μg per animal (Figure 2b). Maximum uptake in tumors was found at an administered mass peptide dose of 1 μg per animal, which was below the estimated ED_{50}. Only minor levels of tracer uptake (30%–40%) remained when the PDL1 epitope was inhibited by administration of NOTA-Nb109 at 100 μg per animal, further indicating the blocking effect of unlabeled NOTA-Nb109.

PET imaging of MC38-hPD-L1 xenografts showed significantly higher accumulation of ^{68}Ga-NOTA-Nb109 at the tumor site and a good delineation of the tumor persisted until the end of imaging session after administration at the dose of 1 μg per animal (Figure 3a). The tumor uptake in different protein dose groups was basically dose-dependent, and was higher than the muscle uptake (Figure 3b). The highest tumor-to-muscle ratio in the 1 μg dose group was approximately 12 (Figure 3c).

In vivo distribution of non-human primates

PET imaging.

As shown in Figure 4 and Figure 5 (a, b), PET scans of cynomolgus monkeys after a single intravenous injection of ^{68}Ga-NOTA-Nb109 showed that the SUV value of the spleen decreased slowly from immediately (0 h) to 4 h post-administration. Radioactive uptake was low in the brain, bone, muscle, stomach and lungs. In the heart and liver, uptake was high immediately after dosing and then decreased rapidly, to approximately 0.9 at 1 h. The SUVs of both kidneys and bladder increased rapidly over time (from about 11–15 to 45–80 during the 4-h test period after administration), indicating metabolism in the kidneys and excreted via urine. As shown in Figure 5 (c), the spleen-to-muscle SUV ratio was approximately 10–12:1 from immediately to 2 h after administration, and this ratio increased to approximately 20.6 due to the decrease in the background SUV in muscle at 4 h after administration.

Dosimetry studies.

Organ-absorbed doses were estimated according to the cynomolgus monkey ^{68}Ga-NOTA-Nb109 biodistribution data at different time-points using OLINDA2.1 software and extrapolated to estimate the adult male equivalent. The organ-absorbed doses are summarized in Figure 5(d). The effective dose was estimated at 0.0226 mSv/MBq; therefore, a proposed patient dose of 185 MBq ^{68}Ga-NOTA-Nb1069 would yield a radiation dose of 4.1 mSv.

Pharmacodynamics.

The correlation coefficients between the serum concentration (ng/mL) analyzed by ELISA and ex vivo blood radioactivity (%ID/g) or heart uptake (in vivo) were 0.985 and 0.997, respectively, indicating strong correlations among the serum concentration, blood, and heart uptake (%ID/g) (Supplemental Figure 2a-f). Hence, the in vivo pharmacokinetics (PK) of drug metabolism can be monitored by both in vitro methods (serum radioactivity ID%/g detection or blood SNA002 protein concentration) and in vivo methods (heart SUV). 〔Pharmacokinetics parameters were shown in Supplemental Table 1〕

Serum intact ^{68}Ga-NOTA-Nb109 signals were detected by radio-HPLC at 15 min and 30 min post-dose. The radioactive signal was negligible at 1 h after administration, indicating rapid metabolism and a high fraction presentence with parental ^{68}Ga-NOTA-Nb109 (Supplemental Figure 3). Furthermore, this conclusion was confirmed by the absence of signals for serum free NOTA detected by LC-MS.

Discussion

Immunotherapy is a valuable treatment strategy for cancers, especially the immune checkpoint PD-1/PD-L1-based immunotherapy [20, 21]. However, the curative effect of anti-PD-1/PD-L1 therapy is closely related to PD−L1 expression level [22]; therefore, the desired response is not achieved in all patients [20, 23]. Consequently, monitoring of tumor-based PD-L1 biomarkers has provided an important reference for therapeutic selection and prediction of the response to targeted therapies.

Previous studies [18, 19] have confirmed that the tracer ^{68}Ga-NOTA-Nb109 is suitable for specific targeting of endogenous PD-L1 and real-time detection and quantification of PD-L1 expression in different types of cancer. To further clarify the influence of the protein mass on this tracer, we designed a series of studies to explore the biodistribution of ^{68}Ga-NOTA-Nb109 at different masses in tumor-bearing nude mice and humanized mice, and confirmed the selected dose in non-human primates.

The injected protein mass (Nb109) has an influence role on the uptake of ^{68}Ga-NOTA-Nb109 in normal organs and tumor tissues. In nude mice, the A375-hPDL1 tumor-to-muscle ratio in the 0.3−10 μg/animal dose group was approximately 2.5−3.5 times greater than that in 100 μg/animal, indicating ^{68}Ga-NOTA-Nb109 has a better target-to-background ratio at low doses. As there is no cross-reactivity between mouse hPDL1 and Nb109 (data not shown), only the binding to A375-hPDL1 tumors was regarded as specific.

The non-specific uptake in other organs was influenced by the protein mass, and a dose-related target-to-background uptake ratio was identified. The strategy of adding unlabeled proteins into tracers to change the non-specific binding in non-target organs was also adopted using ^{68}Ga-NOTA-2Rs15d in a previous study, which showed increasing specific uptake of the radioactive probe in the tumor and decreased non-specific uptake in normal organs (lungs, spleen, liver) with increasing mass of the "cold" protein from 0.1 to 10 mg [24].

Due to the high non-tumor (i.e., lymphoid tissue) expression of PD-L1, the effect of the specific binding of other normal organs on the target-to-background ratio should not be underestimated. Therefore, we further explored the influence of differences in protein mass on distribution in hPD-L1 transgenic mice using the similar dose with that mentioned above. The tumor-to-normal organ ratios decreased as the cold mass administered increased. Maximum uptake in tumors occurred after administration of 1 µg/per animal, which was similar to the dose range observed in nude mice. These observations indicated that tumor uptake is improved at doses below the estimated ED_{50}. In hPD-L1 transgenic tumor-bearing mice, the ^{68}Ga-NOTA-Nb109 uptake in normal tissues serves as a surrogate model of the activation state of the immune system. A dose escalation (0–500 µg) study using another PD-L1 tracer, [89]Zr-DFO-6E11, co-injection with 6E11 increased the relative tumor uptake and decreased the splenic uptake [25].

Based on the protein mass dose of 1 µg/per animal in humanized mice and an estimated body weight of each mouse of 20 g, the mouse-monkey dose conversion factor (mg/kg) was 0.25; therefore, the recommended dose for cynomolgus monkey was 12.5 µg/kg. Hence, we conducted PET/CT imaging in a cynomolgus monkey to further verify the in vivo specific binding of ^{68}Ga-NOTA- Nb109 at the dose of 15µg/kg. Major uptake was detected in the spleen although the highest uptake was detected in kidneys and urinary bladder. There was no obvious uptake in other tissues 30 min post-dose. Some studies have indicated high PDL1 expression in the spleen [26, 27]; therefore, the specific uptake in the spleen of cynomolgus monkeys indicates that ^{68}Ga-NOTA-Nb109 binds monkey PD-L1 specifically and can be used for effective measurement of PDL1 expression in primates *in vivo.* The high spleen-to-muscle ratio further confirmed the specificity, indicating that ^{68}Ga-NOTA-Nb109 data obtained in non-human primates will provide reliable information for predicting future applications in humans. The high uptake in the kidneys and bladder is attributed to the metabolism and excretion of ^{68}Ga-NOTA-Nb109. This result is consistent with previous reports which ascribe the high signals of nanobodies in the kidney to their clearance from the blood via the urine [7]. The characteristics of urine production may be a commonality of the low molecular weight protein or other molecules, such as WL12 (a ^{64}Cu-labled peptide that binds with low nM affinity to human, but not to mouse PD-L1), NOTAZPD-L1_1 (affibody molecule with affinities of 1 nM for human and rhesus PD-L1) [28] and the ^{18}F-labeled anti-PD-L1 adnectin (^{18}F-BMS-986192, approximately 10 kD) [29].

Non-human primates are the ideal model of the human system; therefore, the absorbed dose was estimated based the biodistribution in cynomolgus monkey. The dose-limiting organ in adult male human patients is the urinary bladder wall (0.29 mSv/MBq). The estimated absorbed dose converted from the

male cynomolgus monkey to the adult male was 0.023 mSv/MBq (effective dose). The recommended dose of ^{68}Ga-NOTA-Nb1069 for clinical trials is approximately 185 MBq (5 mCi), which generates an effective dose of approximately 4.1 mSv. This absorbed dose is similar to the effective dose of ^{68}Ga-NOTA-2Rs15d [24] (4 mSv for 185 MBq of administered activity) but lower than the effective dose of standard ^{18}F-FDG [30] measured by PET scanning (7 mSv for 370 MBq of administered activity) and much lower than that of a ^{89}Zr-labeled antibody [31] measured by PET scanning (40 mSv for 74 MBq). Thus, these data indicate that the ^{68}Ga-NOTA-Nb109 can be regarded as safe for clinical diagnostic translation.

In previous studies, the high stability of ^{68}Ga-NOTA-Nb109 was confirmed by its integrity in physiologic media and human serum (**Supplemental Fig. 1**). Furthermore, we have proved the binding affinity to hPD-L1 and the metabolic characteristics of Nb109 in vivo were affected by neither the NOTA chelator conjugation nor Ga complexation in other studies (data not shown). The good consistency among heart SUV, serum radioactivity (ID%/g), and serum Nb109 protein concentration demonstrated that the *in vivo* PK of drug metabolism can be monitored by both *in vitro* methods (serum radioactivity ID%/g detection or blood Nb109 protein concentration monitoring) and *in vivo* methods (SUV of the heart). This would be important for clinical translation in the future.

Although the relationship between PD-L1 level and the radioactive uptake has not been thoroughly investigated, previous studies [18, 19] have indicated that ^{68}Ga-NOTA-Nb109 accumulation accurately reflects the dynamic changes of PD-L1 in real time. However, this remains to be confirmed in future studies.

Conclusion

^{68}Ga-NOTA-Nb109 showed specific accumulation in xenografts in ex vivo biodistribution studies and in monkey PET/CT imaging. Based on the dose escalation distribution data, we recommended a dose range for further clinical use, and monkey dosimetry studies confirmed the safety of the tracer. Further quantitative studies may be required for the clinical translation of ^{68}GaNOTA- Nb109.

Abbreviations

PET/CT: positron emission tomography/computed tomography; PD-1: programmed cell death protein 1; IHC: immunohistochemical; mAbs: monoclonal antibodies; KD: equilibrium dissociation constant; NOTA: 1,4,7- triazacyclononane-1,4,7-triacetic acid; HPLC: High performance liquid chromatography; TLC: thin layer chromatography; ELISA: enzyme-linked immunosorbent assay; DAR: Drug-to-antibody ratio; %ID/g: percentage of injection dose per gram of tissue; ROI: region of interest; SUV: standard uptake value; ED_{50}: estimated half-maximal effective dose; T/M: tumor-to-muscle; PK: pharmacokinetics;

Declarations

Acknowledgments

Author Contributions

YLY and CW designed the study, and YLY performed all experiments and wrote the

manuscript. YS assisted in the cell culture, characterization of Nb109 and NOTA conjugation Nb109 and enzyme-linked immunosorbent assay. CW labeled Nb109 with ^{68}Ga and performed part of the in vivo experiments. TX and XH helped to revise the manuscript. HX, HYF, DQC and FZ supervised the project and provided the funding acquisition. All authors have reviewed and approved the manuscript.

Funding

Data Availability Statement

All data generated or analysed during this study are included in this published article [and its supplementary information files].

Ethics approval

Animal use procedures were in accordance with the recommendations of the European regulations (EU Directive 2010/63) approved by the Laboratory Animal Use and Management Committee of Jiangsu KMQ Biotech Co., Ltd. (IACUC No.: KMQ-CLI001001 for non-human primate study) and Suzhou GenePharma Co., Ltd. (IACUC No.: 2020265 for mouse study).

Conflicts of Interest

None of the authors have any conflicts of interest to declare.

Author details

[1]School of Pharmacy, Yantai University, 30 Qingquan Road, Laishan, Yantai, Shandong, China

[2]SmartNuclide Biopharma Co. Ltd, 218 Xinghu St., BioBAY A4-202, Suzhou Industrial Park, China

[3]Zhejiang Provincial Key Laboratory of Pancreatic Disease, The First Affiliated Hospital, School of Medicine, Zhejiang University, Hangzhou, China

[4]Department of Hepatobiliary and Pancreatic Surgery, The First Affiliated Hospital, School of Medicine, Zhejiang University, Hangzhou, China

References

1. Bray, F., et al., Global cancer statistics 2018: GLOBOCAN estimates of incidence and mortality worldwide for 36 cancers in 185 countries. CA Cancer J Clin, 2018. 68(6): p. 394-424.

2. Organization, W.H., WorldCancer report 2020. p. 352.

3. Love, C., et al., FDG PET of infection and inflammation. Radiographics A Review Publication of the Radiological Society of North America Inc, 2005. 25(5): p. 1357.

4. Jagoda, E.M., et al., Immuno-PET Imaging of the Programmed Cell Death-1 Ligand (PD-L1) Using a Zirconium-89 Labeled Therapeutic Antibody, Avelumab. Molecular Imaging, 2019. 18(22): p. 153601211982998.

5. Bensch, F., et al., 89Zr-atezolizumab imaging as a non-invasive approach to assess clinical response to PD-L1 blockade in cancer. Nature medicine, 2018.

6. Niemeij Er, A.N., et al., Whole body PD-1 and PD-L1 positron emission tomography in patients with non-small-cell lung cancer. Nature Communications, 2018. 9(1).

7. Broos, K., et al., Non-invasive assessment of murine PD-L1 levels in syngeneic tumor models by nuclear imaging with nanobody tracers. Oncotarget, 2017. 8(26): p. 41932-41946.

8. Wissler, H.L., et al., A Site-Specific ImmunoPET Tracer to Image PD-L1. Molecular Pharmaceutics, 2019.

9. Stutvoet, T.S., et al., Molecular imaging of PD-L1 expression and dynamics with the adnectin-based PET tracer 18 F-BMS-986192. Journal of Nuclear Medicine, 2020. 61(12): p. jnumed.119.241364.

10. A, S.C., et al., Rapid PD-L1 detection in tumors with PET using a highly specific peptide. Biochemical and Biophysical Research Communications, 2017. 483(1): p. 258-263.

11. Abousaway, O., et al., Noninvasive Imaging of Cancer Immunotherapy. Nanotheranostics, 2021. 5(1): p. 90-112.

12. Nimmagadda, S., Quantifying PD-L1 Expression to Monitor Immune Checkpoint Therapy: Opportunities and Challenges. 2020.

13. Irina, et al., In vivo binding of [68Ga]-DOTATOC to somatostatin receptors in neuroendocrine tumours — impact of peptide mass. Nuclear Medicine and Biology, 2010.

14. Velikyan, I., et al., Good manufacturing practice production of [68Ga]Ga-ABY-025 for HER2 specific breast cancer imaging. American Journal of Nuclear Medicine & Molecular Imaging, 2016. 6(2): p. 135.

15. Josefsson, A., et al., Imaging, Biodistribution, and Dosimetry of Radionuclide-Labeled PD-L1 Antibody in an Immunocompetent Mouse Model of Breast Cancer. Cancer Research, 2016. 76(2): p. 472.

16. Kumar, D., et al., Peptide-based PET quantifies target engagement of PD-L1 therapeutics. The Journal of clinical investigation, 2018. 129(2).

17. Chakravarty, R., S. Goel, and W. Cai, Nanobody: the "magic bullet" for molecular imaging? Theranostics, 2014. 4(4): p. 386-98.

18. Liu, Q., et al., Immuno-PET imaging of (68)Ga-labeled nanobody Nb109 for dynamic monitoring the PD-L1 expression in cancers. Cancer Immunol Immunother, 2021.

19. Lv, G., et al., PET Imaging of Tumor PD-L1 Expression with a Highly Specific Nonblocking Single-Domain Antibody. J Nucl Med, 2020. 61(1): p. 117-122.

20. Broos, K., et al., Noninvasive imaging of the PD-1:PD-L1 immune checkpoint: Embracing nuclear medicine for the benefit of personalized immunotherapy. Theranostics, 2018. 8(13): p. 3559-3570.

21. Natarajan, A., et al., Novel Radiotracer for ImmunoPET Imaging of PD-1 Checkpoint Expression on Tumor Infiltrating Lymphocytes. Bioconjug Chem, 2015. 26(10): p. 2062-9.

22. Chatterjee, S., et al., Rapid PD-L1 detection in tumors with PET using a highly specific peptide. Biochem Biophys Res Commun, 2017. 483(1): p. 258-263.

23. Geng, Q., et al., PD-1/PD-L1 Inhibitors for Immuno-oncology: From Antibodies to Small Molecules. Curr Pharm Des, 2018. 23(39): p. 6033-6041.

24. Catarina, et al., Synthesis, preclinical validation, dosimetry, and toxicity of 68Ga-NOTA-anti-HER2 Nanobodies for iPET imaging of HER2 receptor expression in cancer. Journal of Nuclear Medicine Official Publication Society of Nuclear Medicine, 2013.

25. Christensen, C., et al., Quantitative PET imaging of PD-L1 expression in xenograft and syngeneic tumour models using a site-specifically labelled PD-L1 antibody. Springer Open Choice, 2019. 47(5).

26. Bensch, F., et al., 89Zr-atezolizumab imaging as a non-invasive approach to assess clinical response to PD-L1 blockade in cancer. Nature Medicine, 2018. 24(12): p. 1852-1858.

27. Freeman, G.J., et al., Engagement of the PD-1 immunoinhibitory receptor by a novel B7 family member leads to negative regulation of lymphocyte activation. J Exp Med, 2000. 192(7): p. 1027-34.

28. Gonzalez Trotter, D.E., et al., In Vivo Imaging of the Programmed Death Ligand 1 by (18)F PET. J Nucl Med, 2017. 58(11): p. 1852-1857.

29. Donnelly, D.J., et al., Synthesis and Biologic Evaluation of a Novel 18 F-Labeled Adnectin as a PET Radioligand for Imaging PD-L1 Expression. Journal of Nuclear Medicine, 2017. 59(3): p. jnumed.117.199596.

30. Brix G, L.U., Glatting G, et al., Radiation exposure of patients undergoing whole-body dual-modality 18F-FDG PET/CT examinations. Nuklearmedizin, 2014. 53(05): p. 217-220.

31. Brjesson, P.K.E., et al., Radiation Dosimetry of Zr-89-Labeled Chimeric Monoclonal Antibody U36 as Used for Immuno-PET in Head and Neck Cancer Patients. Journal of Nuclear Medicine, 2009. 50(11): p. 1828-1836.
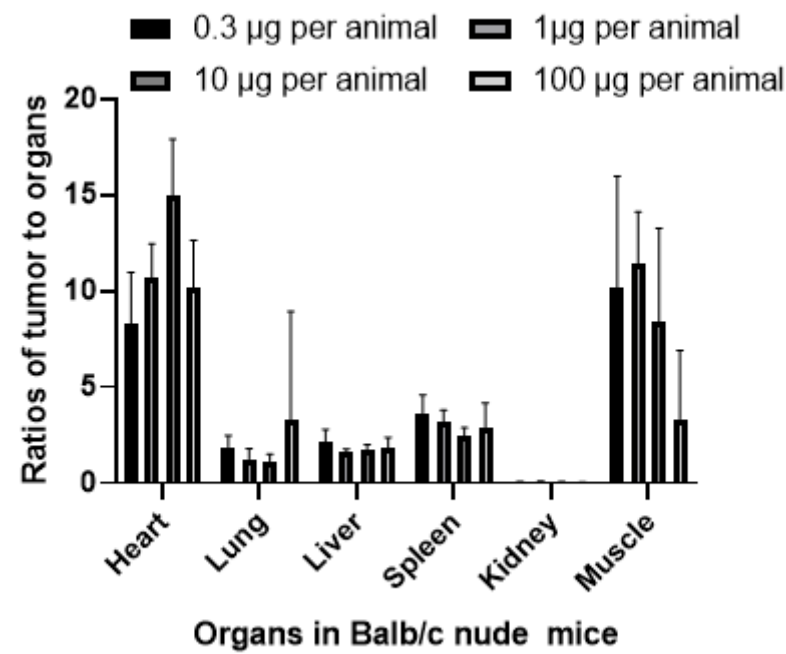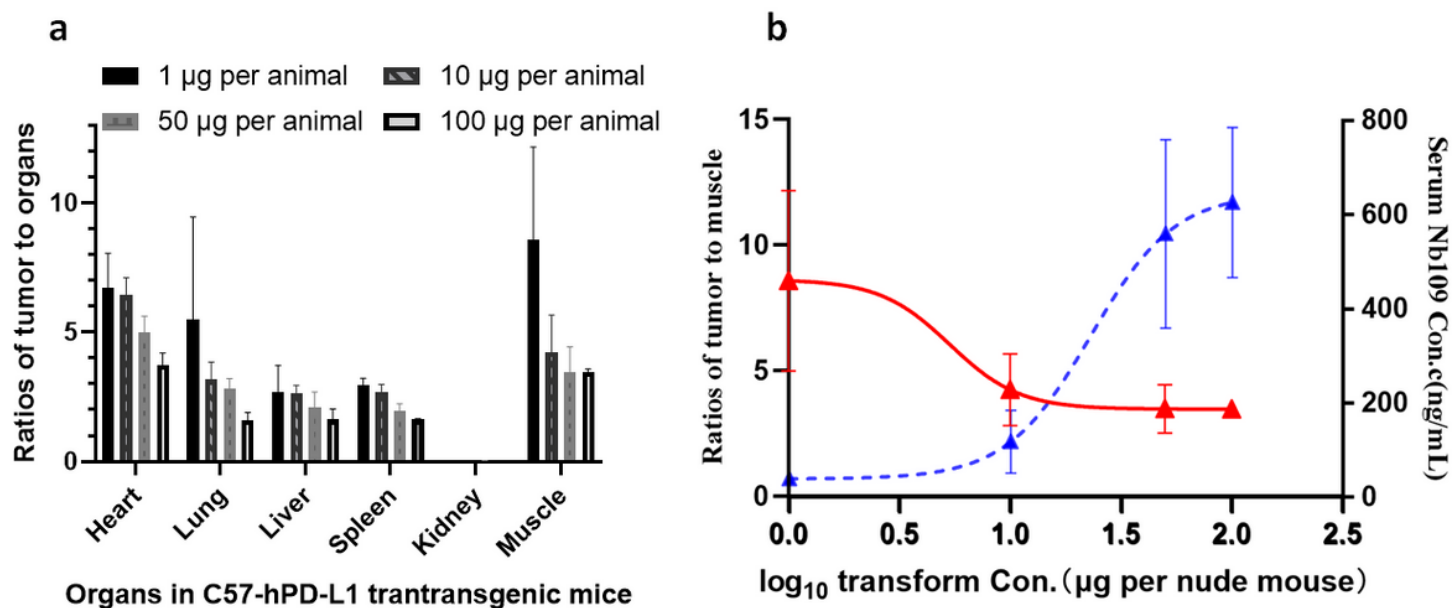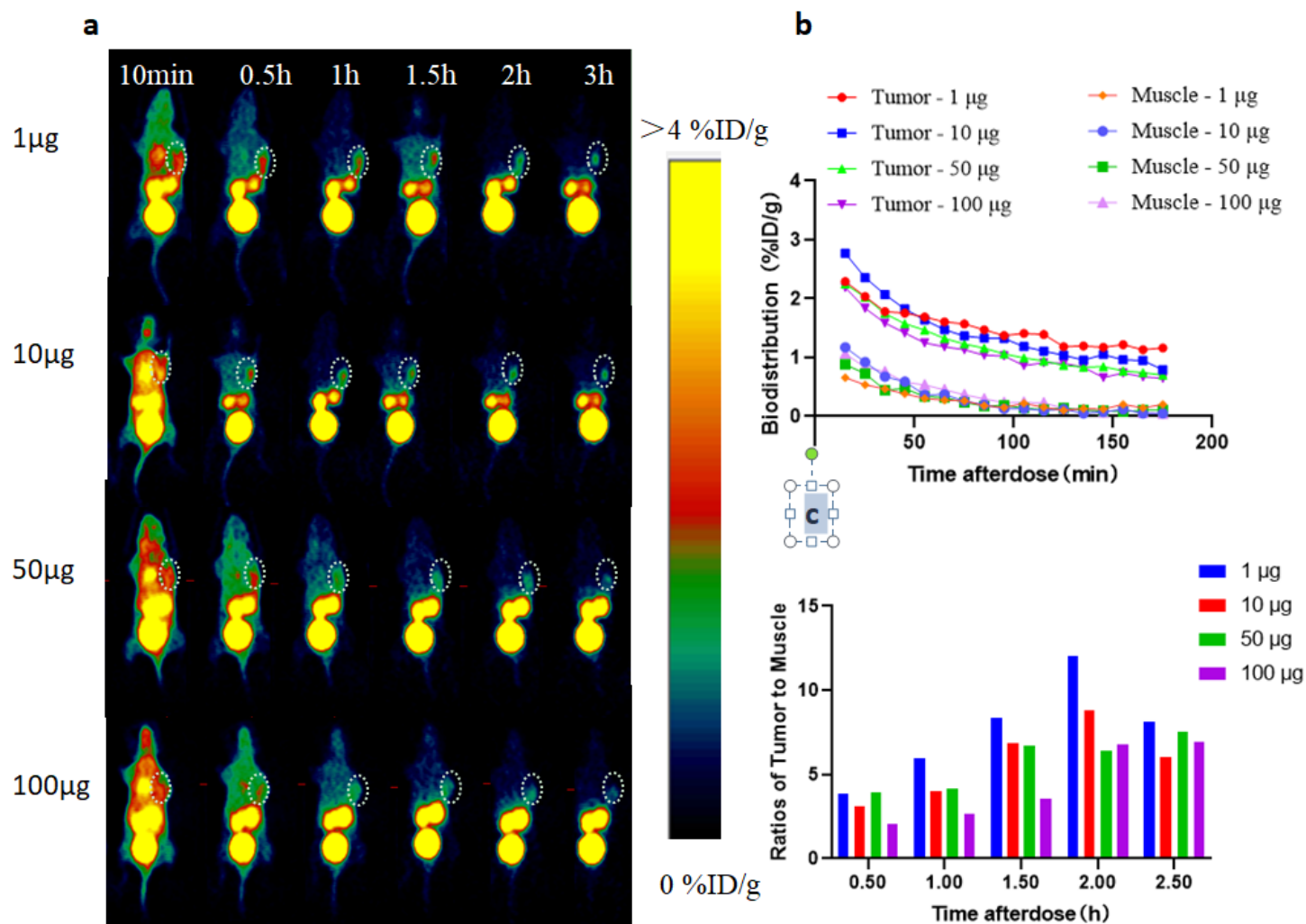
Figures

Figure 1

Tumor-to-organ ratios for different masses of 68Ga-NOTA-Nb109. The tracers were administered to Balb/c A375-hPDL1-tumor-bearing nude mice (left, n = 6) at 1.5 h after injection. Data represent the mean ±SD.
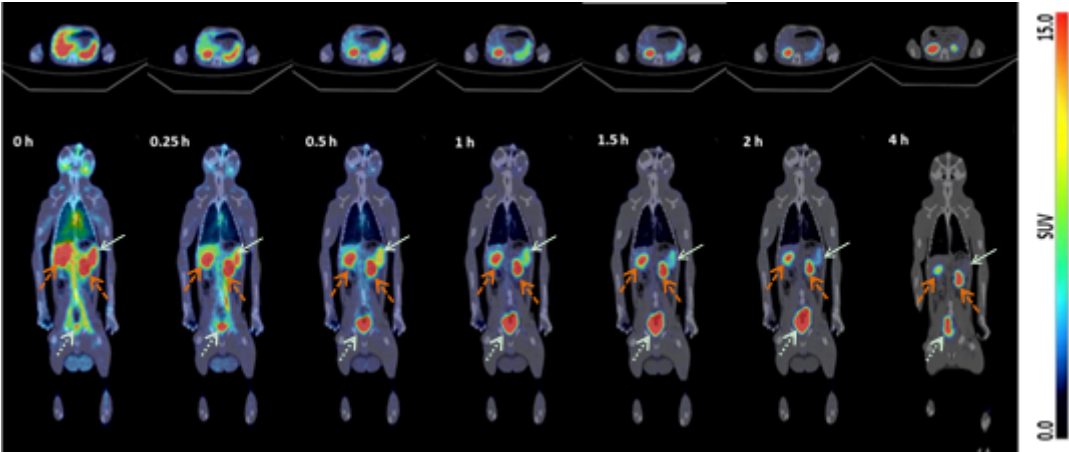
Figure 2

(a) Tumor-to-organ ratios for different masses of 68Ga-NOTA-Nb109. The tracers were administered to C57-hPD-L1 transgenic MC38-hPDL1-tumor-bearing mice (n = 3) at 1.5 h after injection. (b) Fitting curves of tumor-to-muscle ratios or serum Nb109 concentration.
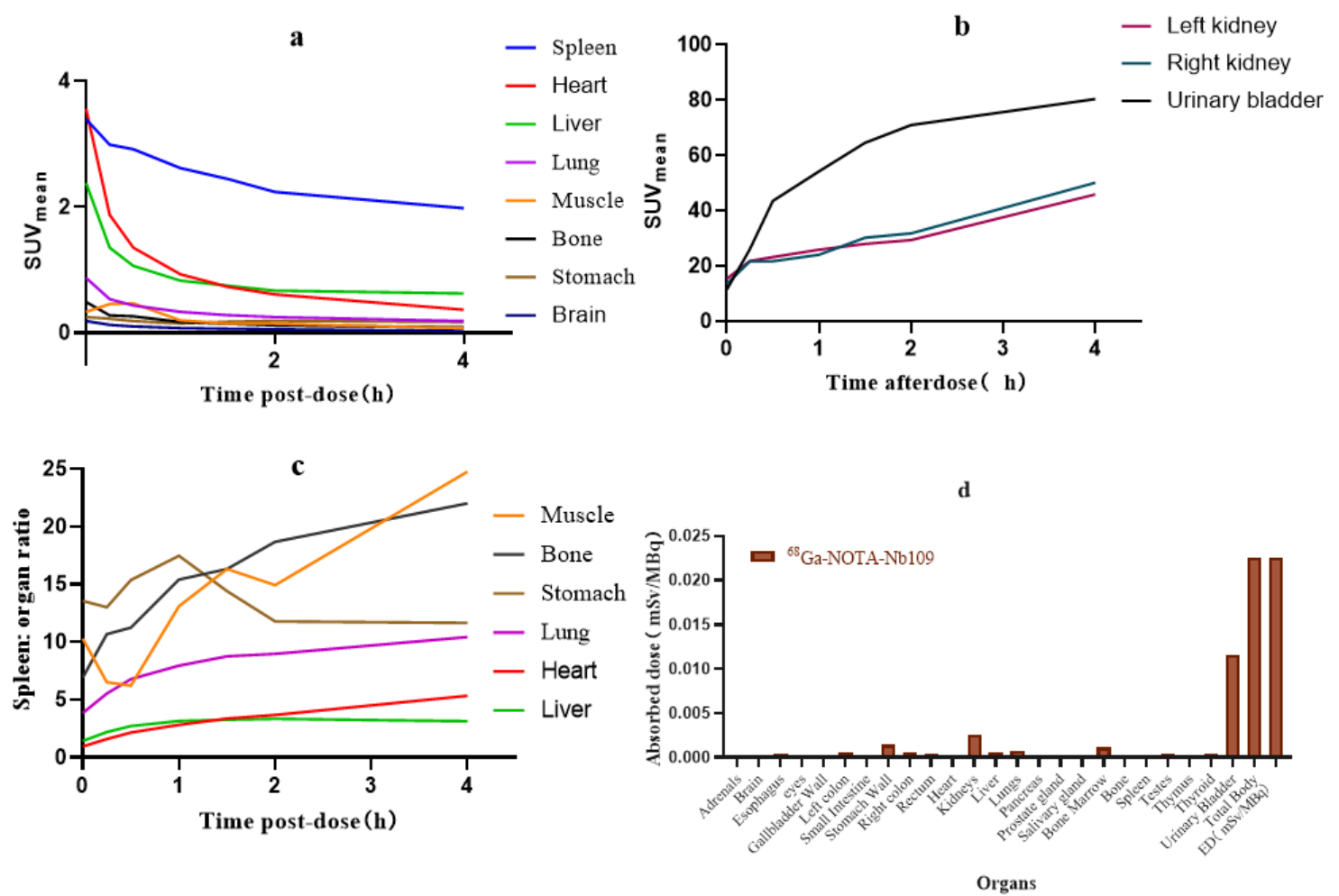
Figure 3

(a) Dynamic microPET imaging of 68Ga-NOTA-Nb109 in C57-hPD-L1 tumor-bearing transgenic mice over 0–3 h. (b, c) Biodistribution of 68Ga-NOTA-Nb109 and tumor-to-muscle (T/M) ratio analyzed by quantification analysis of PET image. The white dotted circle indicates the tumor.

Figure 4

PET/CT images of a healthy cynomolgus monkey at different time-points after injection of 68Ga-NOTA-Nb109. Below: coronal tomograms; above: transverse tomograms. The white arrow indicates the spleen, the white dotted line indicates the bladder, and the red dotted line indicates the kidneys.

Figure 5

Radioactivity in the ROI in images of cynomolgus monkeys was quantified as SUV mean. (a) Time-activity curves of the spleen, heart, liver, lung, muscle, bone, stomach and brain; (b) Time-activity curves of the kidneys and urinary bladder; (c) Spleen:organ (heart, liver, lung, muscle, bone, stomach and brain) ratios curves at different time-points; (d) Effective Dose estimation from cynomolgus monkeys to adult humans (mSv/MBq).

Supplementary Files

This is a list of supplementary files associated with this preprint. Click to download.

- Supplementarymaterial.docx